III. R & D RELATED TO A FUTURE RARE ISOTOPE ACCELERATOR FACILITY

OVERVIEW

The Rare Isotope Accelerator (RIA), a next-generation facility for basic research in nuclear physics, is a high priority for construction in the United States by the Department of Energy. The overall concept for RIA was developed during 1999 by the ISOL Task Force, a sub-committee of the Nuclear Science Advisory Committee (NSAC). A preliminary cost analysis of the RIA project was developed jointly by Argonne National Laboratory and the National Superconducting Cyclotron Laboratory of Michigan State University. The costs were reviewed by another sub-committee of NSAC in January, 2001. Based on this analysis and review the estimated construction cost (TEC) for RIA is $644M in year 2001 dollars. It is possible that construction of RIA could begin in 2004 following various preliminary decisions and site selection. In the meantime, to prepare for construction on this time scale it is essential to continue a vigorous R&D program for RIA. This section is a progress report on the RIA R&D efforts at Argonne.

The RIA R&D topics addressed at Argonne during the year 2000 fall under four main categories: Superconducting Linac Technology, RIA Beam Dynamics, Rare Isotope Production and Separation Technology, and Rare Isotope Beam Diagnostics, sections A-D below.

We have continued to develop and improve the baseline design for the RIA driver linac and also for the RIA post-accelerator. Although specific developments are discussed in subsections of this chapter, we note particularly the following accomplishments:

- Changes in the baseline design for the RIA driver linac were implemented in order to utilize the SC elliptical-cell cavities already developed for the SNS driver linac. This required numerous changes consequent to the shift in frequency for the elliptical cell cavities from 700 MHz to 805 MHz, all of which were generally accepted by a multi-laboratory RIA Driver study group in a meeting organized by Argonne, and held at O'Hare on June 1–2, 2000.

- Numerous improvements in the design of the injector section of the driver linac were initiated to enable the use of two charge states directly from the ECR source, which effectively doubles the beam current available for uranium.

- The design of the low charge state injector for the RIB linac was updated to provide for the post-acceleration of singly-charged beams as heavy as uranium.

- Preliminary designs were developed for the six SC drift-tube cavity types and two cryomodule types required for the RIA driver and post-accelerator in sufficient detail to provide a solid basis for cost estimation.

- An experiment was successfully carried out at ATLAS to demonstrate the viability of the multiple-charge-state mode now proposed for the RIA driver linac.

Several R&D projects for RIA related to isotope production and separation are being pursued. Three of these projects utilize liquid-lithium technology adapted from developments previously carried out for the controlled thermonuclear fusion program. These projects are a hybrid beryllium/lithium target for use at the NSCL at MSU, a windowless flowing lithium target for use with 100-kW uranium beams at RIA, and a flowing thin lithium film to be used as an ion beam stripper in the driver linac of RIA.

Other topics related to rare isotope beam production include further testing and development of the fast gas catcher technology, experiments to validate the simulations of two-step/neutron-generator production schemes, and Monte Carlo diffusion/effusion modeling of conventional ISOL-type target geometries.

A.   SUPERCONDUCTING LINAC TECHNOLOGY

a.1. Drift-Tube Cavity Development (K. W. Shepard, Michael Kelly, and Mark Kedzie)

We have designed a group of six accelerating structures for the drift-tube section of the RIA driver linac which cover the velocity range from .02c to .5c. The structures, shown schematically in Fig III-1, operate at frequencies from 57.5 to 345 MHz. Structures 1 through 4 are similar in parameters to existing superconducting heavy-ion accelerating structures. The two-cell lollipop and spoke loaded structures, numbers 5 and 6 respectively, are in a lesser-explored region of frequency and velocity, so that they are being prototyped first. Figure III-2 shows aluminum models for these cavities which were used to verify numerical simulations and to provide an accurate frequency determination for the final niobium design. Tooling for these prototypes is under construction.

The prototype spoke cavity performance has been significantly improved using our new high-pressure water rinse (see Sec. a.2.). We were able to operate the prototype cw at accelerating fields substantially higher than the design goal for RIA, 5 MV/m.

We have successfully welded niobium to stainless steel, using a thin transition section of vanadium. Although further development is needed (and in progress), this technique will probably permit eliminating the use of explosively-bonded composite materials and simplify fabrication of niobium drift-tube cavities with integral stainless-steel housings.

A 340-350 MHz, 5 kW amplifier, the construction of which was supervised by the Institute for Nuclear Research in Moscow, has been commissioned and is being used in development and testing of niobium cavities for RIA. The use of this amplifier has greatly facilitated the conditioning of the ANL 350 MHz single-cell prototype spoke cavity to field levels well above the design value of 5 MV/m.
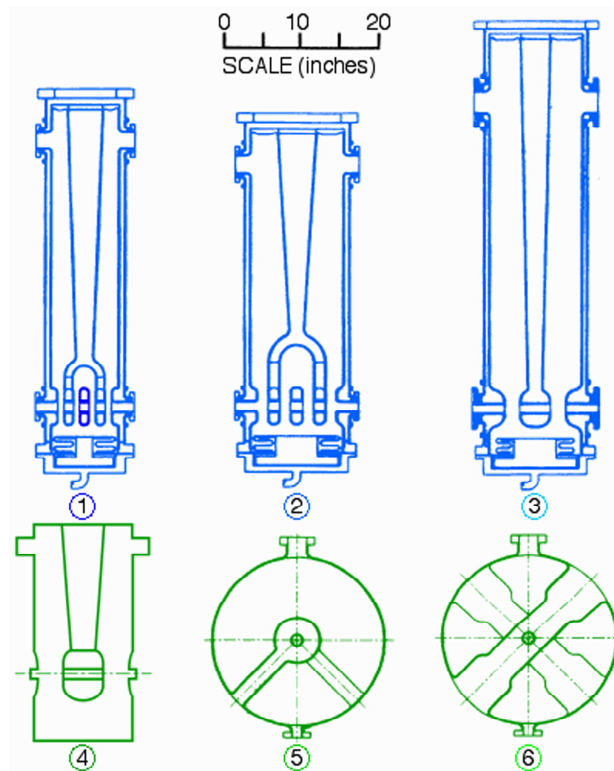

Figure III-1. Six superconducting cavities for the RIA driver linac. Cavities 1 through 3 operate at 57.5 MHz and cover a velocity range from .02c to .1c. Cavity 4 operates at 115 MHz and up to 0.2c. Cavity 5 operates at 172.5 MHz and up to 0.35c. Cavity 6 at 345 MHz and to velocities above 0.5c.

Figure III-2. Aluminum models of the 172 MHz lollipop cavity and 345 MHz spoke cavity being developed for the RIA driver linac.

a.2. Surface Preparation Lab Upgrades (K. W. Shepard, Mark Kedzie and Michael Kelly)

All of the niobium drift-tube superconducting cavities developed to date at ATLAS have been processed by electropolishing. Many of the cavities currently being developed are of geometries that do not permit electropolishing, and must be processed using a buffered chemical polish (BCP) technique. This technique requires tranferring many gallons of a concentrated nitric - hydroflouric acid mixture in or out of a cavity in time period of typically 30 seconds. We have finished the construction of a BCP facility, and following a recent review of all safety issues, have been authorized for operation. Initial tests will be with the prototype spoke cavities being developed for RIA.

A sysem for performing high-pressure (up to 2500 psi) high-purity water rinsing of superconducting cavities has been designed and built (see Fig. III-3). The system removes sub-micron size particulates from the interior surfaces of niobium cavities, improving performance by reducing electron-loading at high field levels. In initial tests, performance of the single-cell prototype spoke cavity was substantially enhanced.
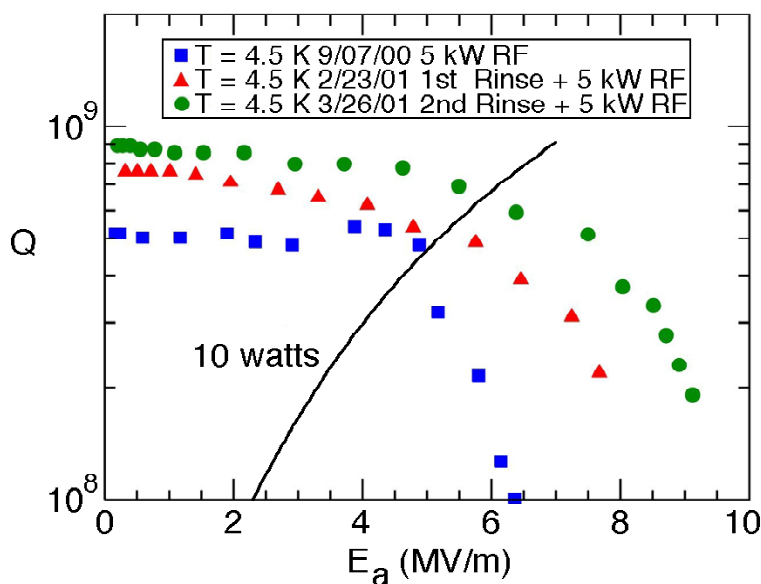
Figure III-3. The business end of the 2500-psi high-pressure water rinsing system being set up on the prototype 350-MHz spoke cavity.

a.3. Drift-Tube Cryomodule Design - (K. W. Shepard, Harold Russell, R. Luther[*])

A design for a 'box' cryomodule for QWR and fork-type cavities was developed by updating and cost-optimizing the cryomodule design used for the ATLAS positive ion injector (PII). A detailed cost estimate of the updated design performed by a potential vendor was used for the recent Harrison committee cost review of the RIA project.

Two alternative designs for a round cryomodule to house the spoke and lollipop type cavities for RIA have been developed. The first design incorporated a monolithic liquid helium container which enclosed 8 cavities, a cooled 'strong-back' for mechanical alignment, and as many as 4 focussing solenoids. The second design was based on several of the best features of the present ATLAS cryostats, i.e., independently-jacketed cavities mounted in a common vacuum for cryostat and beam. Detailed vendor cost estimates indicate the second design to be about 1/3 less costly to fabricate. The second design also appears to be more straightforward to install and maintain.

_____
[*]Meyer Tool & MFG.

a.4. Coupler and Tuner Development (B. Rusnak*, K. W. Shepard)

A major cost item for a RIA driver linac will be the RF systems required to control the phase of the RF fields in the individual superconducting cavities. The cost of the required RF system could be substantially reduced by using a reactive tuning device such as the PIN diode tuners currently used on the ATLAS accelerator. A project has been started to extend the frequency range of such tuners from the present 97 MHz of ATLAS to 350 MHz,and possibly beyond, for use in the RIA driver.

_____

*Lawrence Livermore National Laboratory

a.5. RIA Cryogenics (J. R. Specht)

A spreadsheet was developed tabulating the cryogenic demands for all the superconducting elements of the RIA accelerator. A flow diagram was then developed for each of the four types of cryogenic elements. From this spreadsheet, the flow diagram, and a physical layout of the cryogenic elements, a distribution system was developed to provide the required cryogens to the loads.

Because the RIA facility will use many different superconducting resonator types operating at different frequencies, the temperature of the resonators and heat shields is not consistent for all types. The distribution system developed consists of two coaxial vacuum insulated lines (supply and return) running the length of the linacs. For the supply lines, the inner tube will provide 4.6K 3 bar He for resonator and magnet cooling. The outer concentric tubes will provide heat-shield or VCX cooling (35K @ 5 bar He or 80K @ 3 bar LN_2). The return coaxial lines' center tube will return either 4.6K He @ 1.2 bar or 0.03 bar. Its outer concentric tubes will return either 50K @ 5 bar He or 80K N_2. Using the CEBAF line dimensions, a few pressure drop calculations were made to verify their suitability. Some of the lines will need to be made larger to keep the pressure drops within reason because of the long lengths and increased mass flow requirements of RIA.

Since only the heat of vaporization is used in the LN_2 cryostat circuits, only about half of the available enthalpy is used. This is very inefficient and creates water condensation and ice problems. At RIA the returning cold N_2 gas from the cryostats will be used in the helium refrigerator's pre-cooler. This will solve two problems. It removes the ice and water condensation problems at the cryostats and uses the rest of the available enthalpy saving operating cost.

Because the RIA linacs will operate at variable energies, the cryo-plant must be able to be turned down in order to save operating costs. A refrigeration system was developed to meet these requirements.

A tabulation of the cryogenic requirements for RIA are shown below.

LOAD	Temp (K)	Medium	Min Load (W)	Max Load (W)	Refrigerator Cap. (W)	Margin (%)
Low β Cavities Magnets, Bunchers	4.4	He	1500	3700	5,000	35
High β Cavities	2.0	He	600	5,600	8,600	50
High β heat shields	35	He	10,000	10,000	15,000	50
Magnet Leads	4.4	He	10 g/s	10 g/s	15 g/s	50
Low β Heat Shields, VCX, etc	80	N_2	120 gal/hr	480 gal/hr	-------	-------

Cost estimates were then prepared based on the information gained above. Vendors were contacted to help assure our estimates were reasonable.

B.   RIA BEAM DYNAMICS

b.1. Multiple-Charge Dynamics (K.W. Shepard, P.N. Ostroumov, A.A. Kolomiets[†*])

The principal requirements for the RIA driver accelerator are that it be capable of producing beams of any ion, including uranium, at energies of 400 MeV/nucleon and a total beam power of at least 100 kW. A conceptual design for such a driver linac has been developed, the major elements of which are shown in Fig. III-4. The beam energies shown in Fig. III-4 are for the benchmark uranium beam. Except for the injector RFQ, the entire linac is based on superconducting (SC) accelerating structures, which not only enable cost-effective cw operation, but also have numerous additional advantages for this application. Superconducting ion linacs are configured as an array of short superconducting cavities, each with independently controllable rf phase. Independent phasing allows the velocity profile to be varied: the linac can be tuned to provide higher energies for the lighter ions. For example, the reference design linac can be tuned to provide a uranium beam at an energy of 403 MeV/nucleon and can be re-tuned to provide a proton beam at 899 MeV.
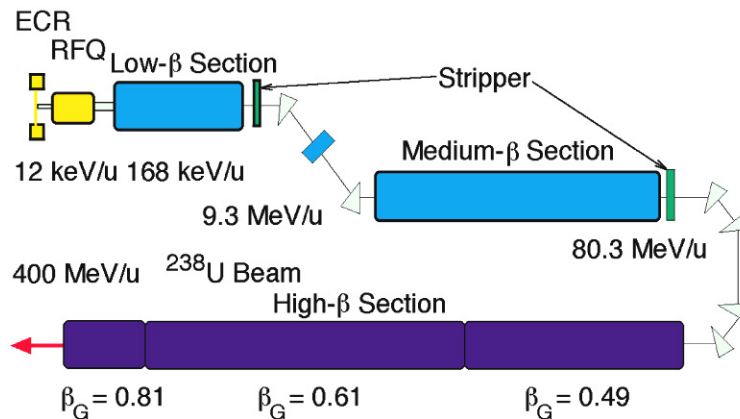

Figure III-4. Elements of the proposed RIA driver linac.

To obtain such broad velocity acceptance, the accelerating cavities are necessarily short, allowing the linac to be configured with ample transverse focussing. Also, since SC structures provide high accelerating gradients, strong longitudinal focussing can be obtained by operating in a phase-focussing mode. We assume a synchronous phase of -30° in the first two superconducting sections, which can be reduced to -25° in the high-β section. In this configuration the SC linac provides very strong focussing, insuring that both transverse and longitudinal acceptances are very large. For example, the longitudinal and the transverse acceptance of high-β section is ~150 times larger than the input beam emittance, which is determined by the ion source and injector RFQ.

Such an immense margin for emittance growth makes possible a novel operating mode for the linac, in which the beam contains multiple charge-states. By simultan-

eously accelerating several of the multiple charge states resulting from stripping the beam, a much higher portion of the stripped beam can be utilized. The increase in efficiency not only provides a substantial increase in the available beam current, but also enables the use of multiple strippers, reducing the size of the linac required for 400 MeV/nucleon beams. A third benefit of using multiple charge states is a reduction in the amount of beam dumped during charge-state selection at the stripping points: this in turn reduces shielding requirements.

Full 3D numerical simulations show such operation to be straightforward, entailing a modest increase of longitudinal and transverse emittance, which remains well within the linac acceptance. Also, it should be noted that the feasibility of multiple charge state beam acceleration has been experimentally established in a series of tests with the existing SC ion accelerator

---

*Institute of Theoretical and Experimental Physics, Moscow, Russia.

ATLAS. For our benchmark design, taking uranium as an example, between the first stripper (9.3 MeV/u) and second stripper (80.3 MeV/u) the beam has an average charge state $q_0 = 71$. In this region we can accelerate 5 charge states, which encompass 70% of the incident beam. After the second stripper, 96% of the beam is in four charge states neighbouring $q_0=89$, all of which can be accelerated to the end of linac. In addition to this enhancement of stripper efficiency, a recent study has shown it possible to accept two charge states of uranium ions from the ECR ion source, additionally doubling the available uranium beam power. By accelerating multiple-charge-state beams of the heavier ions, the available beam current can be increased by as much as a factor of eight. Using these techniques, the RIA driver can produce intense beams of virtually any stable ion using present-day ECR ion sources.

b.2. Demonstration of Simultaneous Acceleration of Multiply Charged Ions Through a Superconducting Linac (P.N. Ostroumov, R.C. Pardo, G.P. Zinkann, K.W. Shepard and J.A. Nolen)

An acceleration of heavy ions at different charge states simultaneously has been proposed and developed. This concept can enhance the utility of high-intensity linacs for heavy ions, where the ions may have to be stripped repeatedly to make optimal use of accelerating fields. Such linacs are being considered for major facilities for nuclear physics research. For example, accelerating on the order of a few times 10^{13} uranium nuclei per second to 400 MeV/u will require two or three stages of stripping. If only one charge state were accepted after each stripping, the intensity at each stage would be reduced by a factor of ~5. A scheme where essentially all the charge states can be accelerated saves ~80% of the beam thus providing up to two order of magnitude more beam at the desired final energy.

A test of this concept with uranium beams was performed at the 50-MV SC linear accelerator at Argonne National Laboratory (the ATLAS accelerator). The details of this test, which demonstrated the viability of this concept for RIA, are reported in the ATLAS section (II.b.2).

b.3. Two-charge State Driver Injector (P.N. Ostroumov, V.N. Aseev[*], A.A. Kolomiets[†])

The front end of the RIA driver linac consists of an ECR ion source, a low energy beam transport (LEBT), a multi-harmonic buncher, a 57.5 MHz RFQ, and, finally, a medium energy beam transport (MEBT) which matches beam into the superconducting linac. We have designed the front end of the driver linac which is capable to accept and simultaneously accelerate two charge states of uranium from an ECR ion source. This mode of operation increases the beam current available for the heaviest ions by a factor of two. The LEBT is designed to select and separate the required ion species and to bunch and match either one or two charge states into the following RFQ structure. The first portion of the LEBT is an achromatic bending-magnet section for charge-to-mass analysis and selection. For the heaviest ions, such as uranium ions, the transport system must deliver to the first buncher a two-charge-state beam with similar Twiss parameters for both charge states. The reference charge state for the design of the LEBT, RFQ and MEBT is 28.5. The RFQ injector is designed to accelerate any beam from protons to uranium to a velocity v/c = 0.01893 at the exit of the RFQ. The ECR is placed on a high voltage platform. The voltage $V_0= 100$ kV is adequate to avoid space charge effects in the LEBT and RFQ and to keep the RFQ length to less than 4 m. A simplified layout of the second part of the LEBT is shown in Fig. III-5. This part of the LEBT solves the following tasks: a) Beam bunching by a four-harmonic external buncher B1 (the fundamental frequency is 28.75 MHz); b) Velocity equalization of two different charge states by the buncher B2, operating at 28.75 MHz; c) Charge-insensitive transverse focusing of the 2-charge state beam and matching to the RFQ acceptance by the electrostatic quadrupoles Q1-Q8. The voltages of the multi-harmonic buncher have been optimised, together with the RFQ parameters, in order to obtain a total efficiency above 80%, while minimizing the longitudinal emittance for each charge state. The second buncher is used to equalize the velocities of the 2 charge states (see Fig. III-5c). The

_____

*Institute for Nuclear research, Moscow, Russia.
†Institute of Theoretical and Experimental Physics, Moscow, Russia

primary design goal for the RFQ is to establish a low output emittance so that the acceleration of multiple-charge-state beams through the rest of the linac becomes straightforward. We performed full 3D simulations of a two-charge-state uranium beam including space charge forces in the LEBT and RFQ, realistic distributions of all electric and magnetic fields along the whole prestripper linac, and the effects of errors, evaluated for

several design options for the prestripper linac. The results indicate that it is possible to accelerate two charge states while keeping emittance growth within tolerable limits. The use of a two-charge state beam is a powerful tool to double the total beam power produced by the heavy ion driver linac.
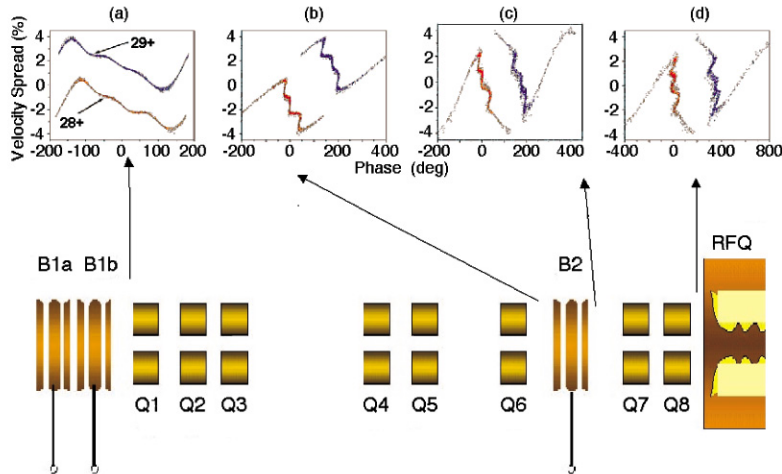

Figure III-5.   Longitudinal phase space plots of two-charge state beam along the LEBT, a) output of the multi-harmonic buncher, b) at the entrance of second buncher, c) after the second buncher, d) at the entrance of the RFQ.

b.4. Layout of a Magnetic Optical System for Transport and Matching of Multiple-Charge-State Heavy-Ion Beams (V. A. Aseev,* J. A. Nolen, P. N. Ostroumov, M. Portillo)

The construction of a high-intensity heavy-ion linac for uranium beams up to 400 MeV/nucleon requires the use of at least two stripping foils to keep the linac total voltage limited to about 1.4 GV. The proposed Rare Isotope Accelerator (RIA) Driver Linac is designed to transport beams of multiple charge states following the stripper foils to keep beam intensity high. In order to avoid beam losses in the high-energy section of the Driver Linac the low-intensity unwanted charge states must be carefully separated and dumped. The beam transport system following the stripping foil must provide simultaneous matching of selected charge states to the six-dimensional acceptance of the following SRF linac. This magnetic transport system (MTS) requires dipole magnets and a rebuncher in order to provide a proper transformation of the 6-dimensional beam emittance. The system must have a dispersive area, effectively operating as a spectrometer. In the region of maximum dispersion, the unwanted charge states are removed by horizontal beam collimation. We have designed such systems for both stripping areas of the driver linac, at 9.3 MeV/u and 80 MeV/u. Several options for MTS design can satisfy the above

requirements. The options chosen seem to best satisfy the overall architectural requirements of the linac. For example, after the first stripper, it is convenient to transversely shift the linac beam axis: the MTS incorporates two 45 degree bends to provide a 4.5 m shift. After the second stripper it is economical to bend the beam through 180°, since such a bend greatly shortens the overall length of the linac tunnel.   The 180° bend provides for high-dispersion regions in the MTS which enable separation of low intensity charge states and cleaning or scraping of any beam halo.

The layout of the MTS following the second stripper is shown in Fig. III-6. For uranium beams, charge states q = 88, 89, 90, 91, and 92 will continue on through the system. Ion trajectory length in this system is independent of the initial beam parameters. For simplicity of design, we assume the beam matrix of the second moments must be the same at the entrance and exit of the system. The reproduction of the second order moments of the beam in the longitudinal phase space is provided for by the rf cavity. All bunches of different charge state must arrive at the rf cavity at the same time

(at the same phase of the rf field). This means that the MTS must have the same path length for all charge states in the initial portion, up to the re-buncher, and also, separately, in the output portion from the rebuncher on. At the final stage of the MTS design, the higher order terms must be included and corrected as

necessary. For this final design stage, numerical simulations of the beam through the MTS were performed including the rebuncher and assuming realistic, non-zero initial emittances in all phase planes. Figure III-7 shows transverse cross-section of multiple-charge state beam at high dispersion area.
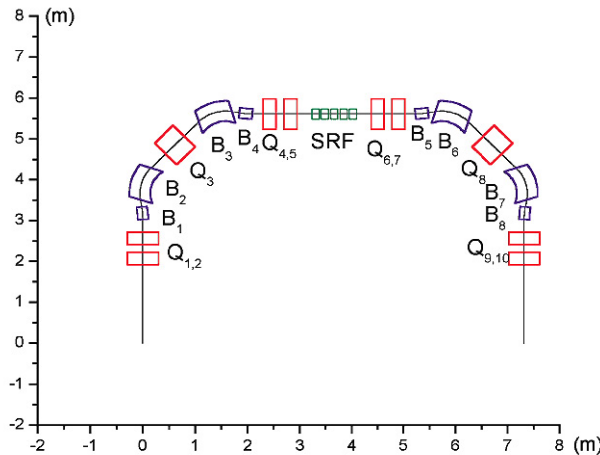
*Institute for Nuclear Research, Moscow, Russia

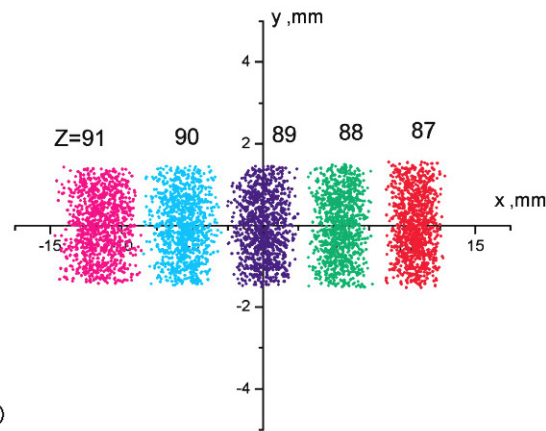Figure III-6. Magnetic transport system for the 180° Bend of multi-Q beam.

Figure III-7. Beam cross section at the entrance of quadrupole lens Q_3.

b.5.. Preliminary Design of the Driver Linac Switchyard (J. Nolen, P. N. Ostroumov, S. Kim*)

Rf deflection of heavy ions beams in RIA Facility is a unique task due to the large beam emittances of the multiple charge state beams. Rf separators and dc septum magnets are required in the beam switchyard that the RIA facility will use for beam distribution to several targets. The most severe condition for operation of the separator will be with multiple-charge-state uranium beam beams. These beams will have largest transverse and longitudinal emittance of any RIA beams. Total momentum spread of the uranium beam exiting the driver linac may be as high as 0.4% due to the effect of phase and amplitude errors of the accelerating field as well as due to the multiplicity of charges. For similar reasons phase width of the uranium bunches may be as much as ~20° at 805 MHz. The relatively large momentum spread will lead to rapid beam debunching. For example, the bunch length will double over a drift distance of 15 m. The use of high frequency rf separators can produce large emittance growth due to the wide bunch width inside the rf separator. A low frequency rf deflector is appropriate for deflection of heavy ion beams. The deflector design can

be based on an H-type rf cavity. Figure III-8 shows a general view of such an rf cavity designed by MAFIA. The fundamental frequency of the bunch sequence is determined by the multiharmonic buncher at the Front End of the driver linac. In two-charge state operation mode all four harmonics are applied and bunch repetition rate will be 57.5 MHz. In a single charge state mode only three harmonics of the multi-harmonic buncher will be used and bunch repetition rate is still 57.5 MHz. Therefore the rf deflector can operate at 115 MHz allowing to split beam intensity to two halves. The length of the electrode is chosen to provide phase slippage 180° inside the cavity for uranium beam. This condition eliminates any effect of fringing fields on uranium beam but produces negligible momentum spread for lighter ions because of higher velocity and smaller phase shift of lighter ion beams. A room temperature rf cavity operating at 115 MHz can provide a maximum electric field on the surface ~20 MV/m in CW mode. We have conservatively designed for a maximum electric field ~6 MV/m between the electrode.

*Advanced Photon Source, ANL

Figure III-8. MAFIA simulatiuons of the H-type cavity for formation of 115 MHz transverse deflecting electric field between the electrodes (red plates on the figure). The arrows represent magnetic field flow. The cylindrical envelope of the cavity is cut to open an internal view.

Table III-I: Basic parameters of the rf deflector for the RIA switchyard.

Maximum electric field	6 MV/m
Effective length	1.0 m
Deflecting angle	± 2 mrad
Characteristic resistance according the MAFIA simulations	3 MOhm
Required rf power (twice of MAFIA prediction)	11 kW

b.6. Low-Charge-State Injector Beam Dynamics (P. N. Ostroumov, A. A. Kolomiets*)

The design goal for the rare isotope beam (RIB) linac is to accelerate heavy ions in the mass range from 6 to 240. , starting with the ions at charge state 1^+. We have designed the injector section of the RIB linac capable to boost an ion beam velocity to the value acceptable by a SC linac. The injector of the RIB linac contains three sections of normally-conducting RFQ. Options for gas stripping with a He cell will be provided at two locations. The output of the first section is at 7 keV/u, and the beams of 66 < mass < 133 will be charge-stripped at this point. Whether stripped or not, ions of any mass and charge state, including mass 240 at charge state 1^+, will be further accelerated by the next section of the 12 MHz RFQ to an energy of 20 keV/u. At this point the beams of mass > 132 will be stripped. Providing two different options for non-equilibrium gas stripping ensures a high efficiency of operation over the full mass range, including mass 240 (see Fig. III-9). The third section of RFQ will operate at 24.25 MHz and accelerate the ions, now at a charge state q/m > 1/66, to an energy of 62 keV/u for injection into the superconducting linac. The multi-harmonic buncher, both 12 MHz RFQ sections, and both He gas-stripper cells will be placed on a 380 kV open-air variable-voltage platform. Placing these elements on a variable voltage platform allows operation with a fixed constant velocity profile for the full mass range of ions, including uranium. Light ions will be accelerated, on exiting the HV platform, above the input matched velocity of the following ground-potential RFQ. To achieve velocity matching for these

ions, a buncher with effective voltage ~60 kV is required.

The RFQ should operate at as low a frequency as is practicable to maximize the transverse focusing strength. As has been demonstrated at ANL the split-coaxial RFQ geometry is appropriate for operation at 12 MHz. The RFQ is designed for a minimum charge to mass ratio of 1/240: ions of higher charge state are accommodated by simply scaling both the platform voltage and the RFQ rf voltage to match. The basic design parameters of three RFQ sections are shown in Table III-II. The acceleration of very low masses may require operation at rf voltages below the linear region of the drive amplifiers, and additional low power rf amplifiers may be required in order to properly stabilize phase and amplitude of the accelerating fields. Numerical simulations of the beam dynamics through the entire chain of RFQ sections have been performed. The proposed design achieves longitudinal emittance as low as 0.2 π keV/u-nsec for 80% of CW beam entering the buncher. A preliminary study shows that beam matching between the RFQ sections, including stripping, is straightforward, and can be achieved without appreciable emittance growth in either the transverse or the longitudinal phase planes. Several rf bunchers are required for the matching purpose. Transverse focusing in the transitions can be done with either electrostatic quadrupoles or SC solenoids. Beam dynamics simulations of each section of the RIB linac injector, using realistic fields, does not show appreciable emittance growth in any section.

---

*Institute of Theoretical and Experimental Physics, Moscow, Russia

Table III-II. Basic Parameters of the RIB linac RFQs.

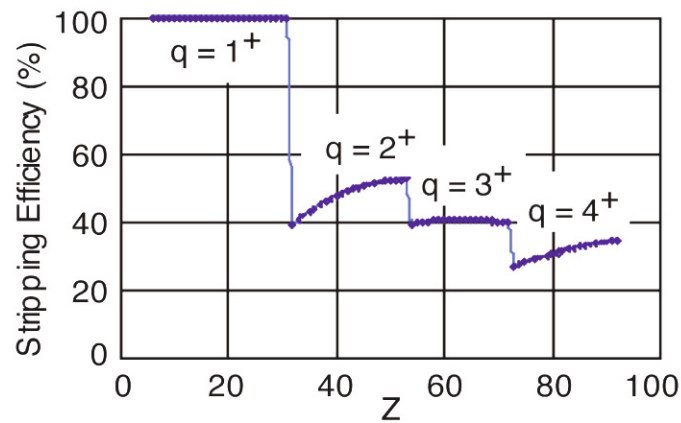| Operating frequency (MHz)	12.125	12.125	24.25
. Charge to mass ratio	1/240	1/240	1/66
Input energy (keV/u)	2.0	7.0	20.0
Output energy (keV/u)	7.0	20.0	61.7
Inter-vane voltage (kV)	92	92	92
Average distance between opposite electrodes (mm)	18	18	18
Maximum electric field (kV/cm)	128	128	128
Modulation	1.3 ÷ 1.9	1.9 ÷ 2.3	1.3 ÷ 2.3
Synchronous phase (deg)	-25	-25	-25
Length (m)	2	4.7	4.25
Transverse normalized acceptance (π·mm·mrad)	0.4	0.3	0.56

Figure III-9. Helium stripping efficiency for the proposed RIB injector section.

b.7. Singly-Charged Heavy-Ion Beam Studies on a 12-MHZ RFQ
(M. P. Kelly, P. N. Ostroumov, K. W. Shepard, B. E. Clifft, and M. Kedzie)

This series of tests successfully completes development of the only existing cw normal conducting RFQ at this low frequency capable of accelerating 1^+ ions over the entire mass range. The RFQ was designed for use in the entrance section of a RIB linac for the RIA (Rare Isotope Accelerator) project[1].

Detailed experimental measurements of singly-charged ^{132}Xe and ^{84}Kr beams accelerated through the RFQ for stable inter-vane voltages up to 90 kV have been performed. As part of an injector to a RIB linac the RFQ would accelerate low energy, low charge-to-mass ratio ion beams with high efficiency (ie. CW operation) while simultaneously introducing negligible transverse or longitudinal emittance growth. We have presented results of a series of measurements[2] using ^{132}Xe and ^{84}Kr beams ranging in energy from 220 to 450 keV injected into the RFQ using the ANL 4 MV Dynamitron and a recently added RF chopper used to simulate pre-bunched beams. Small beam chop widths of a few nanoseconds at the entrance permit detailed tests of the RFQ acceptance and emittance properties. Measured ^{132}Xe and ^{84}Kr energies at the RFQ exit are in agreement with model calculations. The long term thermal stability of the RFQ at the highest inter-vane voltages (~100 kV) was also explored.

A typical time-versus-energy spectrum showing bunches spaced by 160 ns centered at the expected energy of 1 MeV is shown in Figure III-10, top panel. The energy width is dominated by the detector resolution as these low energies. The bottom panel is the time projection indicating bunch widths ~15 nanoseconds. Accelerated beam energies and the behavior of the RFQ as a function of vane voltage and the injected bunch phase are all in agreement with simulations.

This RFQ after refitting with new copper vane tips modulated for masses up to uranium and including direct water cooling will be entirely suitable for use in the entrance section of a RIB linac for RIA.

---

[1]The US RIA Project, G. Savard, 2001 Particle Acclerator Conference, June 18-22, (2001).
[2]Singly-Charged Heavy-Ion Beam Studies on a 12 MHz RFQ, M.P. Kelly, P.N. Ostroumov,
K.W. Shepard, B.E. Clifft, M. Kedzie, 2001 Particle Acclerator Conference, June 18-22, (2001).
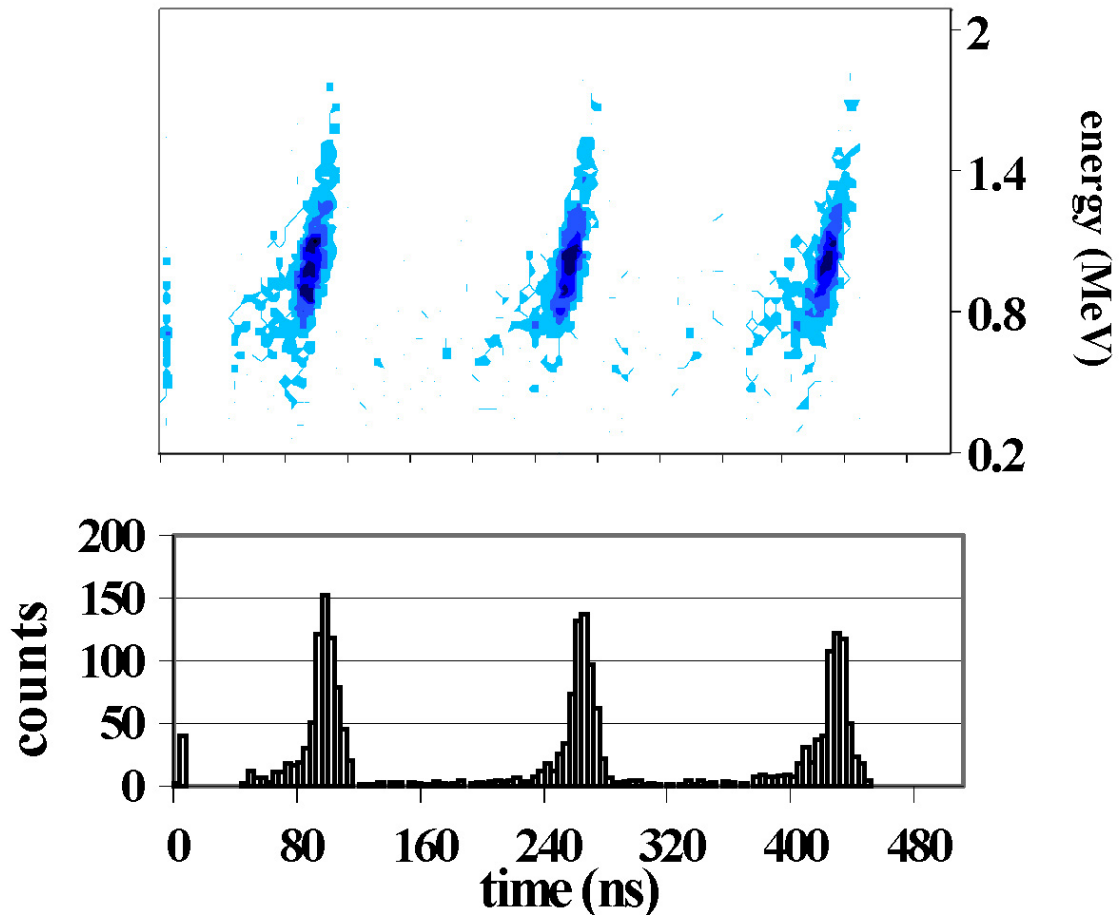
Figure III-10. Time-of-flight versus energy (top) and the time projection (bottom) for accelerated 84Kr at the RFQ exit. The energy spread is dominated by the resolution of the detector for these energies.

C.   RARE ISOTOPE BEAM PRODUCTION AND SEPARATION TECHNOLOGY

c.1.   Development of a Large Accelerated Gas-Cell System for the Collection of Fast Recoiling Radioactive Ions (G. Savard, C. Boudreau*, J. Schwartz, J. Caggiano, J. Clark†, H. Fukutani†, J. Greene, M. Maier[4], T. Pennington, D. Seweryniak, K.S. Sharma†, B. Zabransky)

A large gas cell system was first developed at ATLAS in 1998 for the injection of radioactive ions into the CPT mass spectrometer. It used a large high-purity helium gas volume where fast reaction products separated by the area II gas filled spectrometer were stopped and thermalized as 1+ ions before being extracted by a combination of gas flow and DC and RF electric fields. We proposed at that time that this technique could be extended to the stopping of fragmentation products and led to an important new production mechanism for the proposed RIA facility. We have continued R&D on this technique and are now in the process of developing a full-scale prototype of the RIA gas cell system.

The initial development work performed this year involved construction of a new quarter size cell with similar length to diameter ratio as the envisaged RIA gas cell. This cell was equipped with a new RF-focusing extraction region capable of operating at higher pressure and of a design scalable to the full scale RIA system (see Fig. III-11). This cell, with an inner diameter of about 8 cm and a length of roughly 27 cm, uses only UHV materials. It was installed at the focal plane of the Enge spectrograph in area II. It is separated from the spectrograph vacuum chamber by an all metal 1.9 mg/cm^2 HAVAR window sealed by indium rings and supported by a gold coated tungsten wire grid. The cell is filled with ultra-high purity helium gas fed by an all stainless steel gas system, with the gas purified by a Monotorr purifier (SAES getters Inc.) preceded by a standard cold trap. This cell fits into the existing gas cooler vacuum chamber which was modified to increase the space available and ease alignment of the cell to the gas cooler. The gas cooler was also improved with a clean pump replacing the small roots blower pumping section 2 and improved diagnostics for ions (counting and mass selectivity) and radioactivity.

A number of systematic studies have been undertaken with the gas cell system, looking at the effect of impurities in the gas, gas flow conditions, transmission through the cooler system, efficiency variation with DC and RF parameters inside the cell, etc … While these studies are still ongoing, a few conclusions can already be drawn. The most important conclusion is that the effect of impurities in the gas reduces significantly as the field gradient inside the cell is increased. It appears that the long-range attraction of the ions and impurities does not succeed in bringing together ion and impurity molecules in the presence of the constant collisions which the molecule must undergo to "follow" the ion being dragged in the helium gas. Similarly, the adducts of ion plus helium which are weakly bound are not observed when the electric field becomes significant. Under optimal conditions we find no sign of activity at masses other than those of the radioactive ions being produced.

In the on-line studies, we have created radioactive species and brought them into the cell together with a fraction of the primary beam. This fraction can be varied, although coarsely, by putting different size beam stops at zero degrees or changing other parameters in the reaction or Enge operation. While these studies are still very coarse, we observe saturation effects in the cell which occur at a rate consistent with that we predicted for the point where charge accumulation in the cell will shield the electric field applied. This number is therefore consistent also, when scaled to a cell of the size required for RIA, with the roughly 10^9 ions per second limit we expect to be able to handle with this approach at RIA and which was used for the RIA yield calculations using this extraction system. These studies are clearly very important and to be able to perform them under more controlled conditions we are modifying the Enge spectrograph with the addition of a magnetic triplet and a velocity filter before the dipole magnet. This will give us the ability to continuously vary the amount of primary beam going into the cell for a given amount of radioactive species. With the diagnostics provided by the transmission PPAC installed last year we will then be able to pursue these studies much more quantitatively and with spatial resolution inside the cell.

The next step in the gas cell evolution is a full scale RIA gas cell prototype. A cost efficient design for this cell has been worked out. It will have a stopping length of 0.5 atmosphere-meter of helium and uses a modified RF extraction region capable of providing higher focusing RF fields. This higher-field extraction structure was tested on-line at ATLAS and performed according to specifications. Construction of this new cell is planned to be completed by the fall of 2001 and will be tested first at ATLAS before being moved to the FRS fragment separator at GSI for a full-RIA-energy test. The initial tests at ATLAS will allow us to fully characterize the cell, using the fact that low energy radioactive beams can be stopped at well-defined positions (of the order of a cm diameter) inside the cell. With pulsed beams from ATLAS, the efficiency and time delay in the cell will be studied as a function of the position where the radioactive ions are stopped inside the cell. This will allow to optimize the DC field

geometry to eliminate possible "dead" regions in the cell. Beam time has been approved by the ATLAS PAC for these studies. At the beginning of 2002, the cell will be moved to GSI to be installed behind the FRS fragment separator to operate under conditions similar to those expected at RIA. A nine laboratory collaboration was put together and submitted a proposal to the GSI PAC (proposal S258, spokesperson G. Savard) to study the important aspect of the operation of a gas cell behind a fragment separator, spanning the spectrum from the slowing down of fast heavy ions, to the energy monochromation of the fragment beam to reduce the range straggling, to the final stopping in the cell and extraction. The proposal was reviewed at the December 2000 PAC meeting at GSI and received a large allocation of beam time to pursue this experiment. Initial studies will be performed in the year 2001 and gas cell tests at the high energy should occur in the following year.
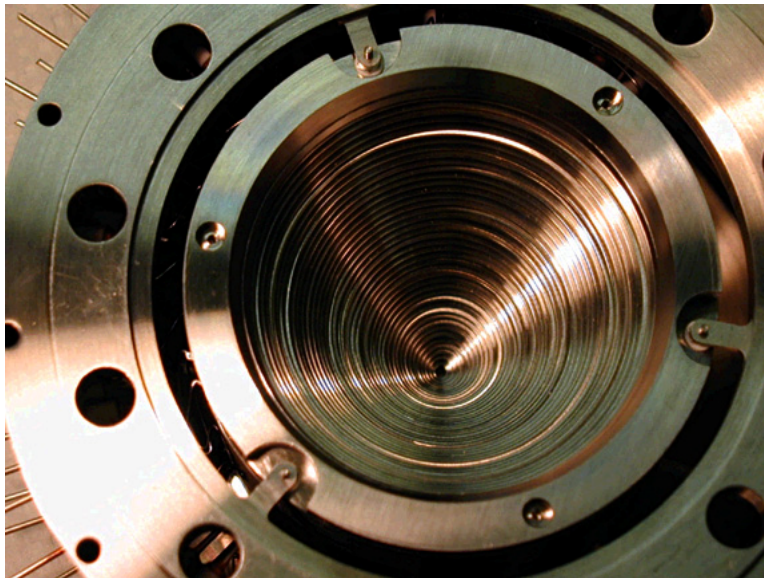
_____
*McGill University
†University of Manitoba
‡GSI

Figure III-11. Photograph of the conical electrodes in the extraction region of the second-generation fast gas catcher.

c.2. **Liquid Lithium Films for Ion Stripping** (J. A. Nolen, C. B. Reed,* A. Hassanein,†
   M. Portillo, J. H. Norem‡)

The RIA Driver Linac design is optimized for accelerating high power uranium beams starting from an ECR ion source at charge state 29. To keep the total linac accelerating voltage relatively low (1.4 GV) two stripping stages are assumed, the first at ~9 MeV/u and the second at ~80 MeV/u for uranium ions. For the final design goal of 400 kW of uranium beam at 400 MeV/u, the beam current at the first stripper location will be ~5 particle microamperes. The stripper foil thickness required for this beam is in the range 200-400 micrograms/cm2. Uranium beams at this intensity will rapidly damage carbon foils even if they are mounted on a large rotating wheel. At this energy, lower atomic number materials such as beryllium or lithium yield higher average charge states and produce less angular scatting than carbon. Hence, we are considering the use of a flowing thin film of liquid lithium at this first stripper location. The technology is similar to that being developed for the thick windowless fragmentation target for the high energy uranium beams, except the thickness must be ~5 micrometers rather than ~2 cm. Calculations indicate that with a 1-mm diameter beam spot on the film the power density is ~15 kW/cm2, but the lithium temperature rise is only ~30 K at a linear velocity of 10 m/s for the lithium. We are currently designing a test facility to house a prototype nozzle to experimentally demonstrate the possibility of producing the required thin and stable liquid lithium film in the required thickness range. A simplified sketch of the concept is shown in Fig. III-12. A liquid lithium stripper can also be used at the second stripper position where a much thicker film can be used and the energy loss is much lower.

*Technology Development Division, ANL
†Energy Technology Division, ANL
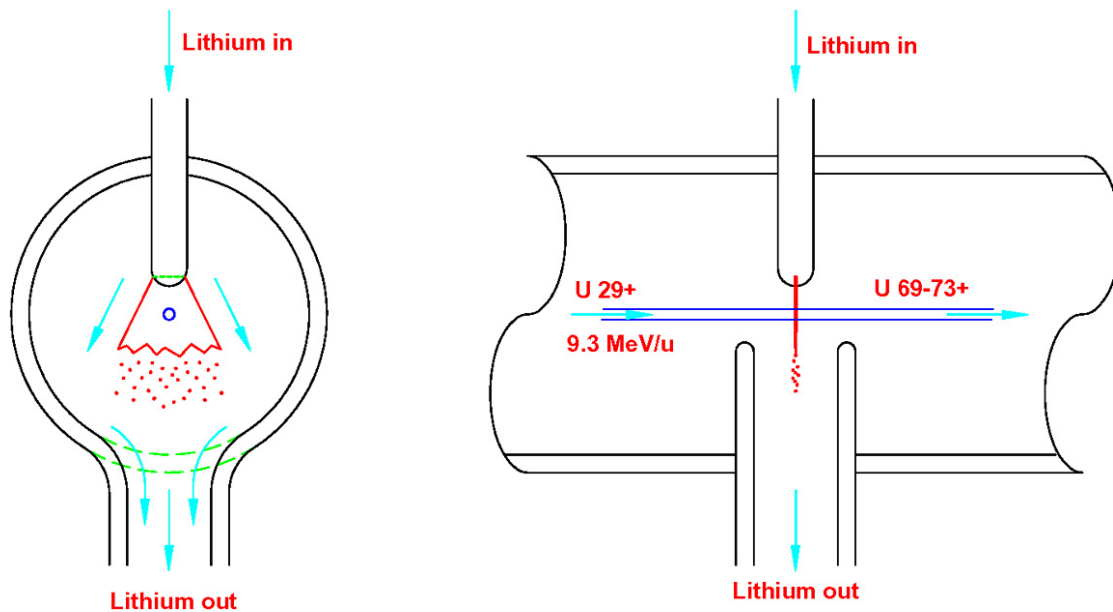‡High Energy Physics Division, ANL

Fig. III-12. A simplified sketch of the liquid lithium film ion beam stripper concept.

c.3   Liquid Lithium for High Power Density Fragmentation Targets (J. A. Nolen, C. B. Reed,* and A. Hassanein,† D. J. Morrissey,‡ J. H. Ottarson,‡ and B. M. Sherrill,‡)

Windowless liquid lithium targets for in-flight fragmentation or fission of high-power heavy-ion beams are being developed for the U.S. RIA project. With uranium beam power of 100 kW and a beam-spot diameter of 1 mm, the power density in the target is over 1 MW/cm3. Thermal analysis for this example indicates a very low peak temperature for the lithium when flowing at a linear velocity of 10 m/s. A vacuum test chamber is under construction at Argonne at an existing liquid lithium facility (ALEX) to demonstrate a 2-cm diameter windowless target. As a first step towards using liquid lithium target technology at a nuclear physics fragmentation facility, a lower power target is being designed and constructed for use at the NSCL. This target will use beryllium windows with flowing lithium. The lithium is part of the target as well as the cooling medium. It is designed for beams between oxygen and calcium with beam power above 3 kW. The tapered beryllium windows are each 1-mm thick for the calcium beams and 7-mm thick for the oxygen beams. The lithium is 5-mm thick. This gives an overall target thickness ranging from about 0.7 g/cm2 to 3 g/cm2 which is adjusted by moving the target vertically. A drawing of the final design for this tapered, hybrid Be/Li target is shown in Fig. III-13. The prototype system will be constructed following design and safety reviews. It will be first checked out at the ANL/ALEX facility and then moved for use with the A1900 fragment separator at the MSU/NSCL.

_____
*Technology Development Division, ANL, †Energy Technology Division, ANL,
‡Michigan State University

Fig. III-13. Drawing of the hybrid lithium/beryllium target with an overall thickness range from 0.7 g/cm2 to 3 g/cm2. The target body is beryllium and the lithium flows through the 5-mm thick channel. (The drawing is dimensioned in inches.)

c. 4.   Optimization Of ISOL Targets Based On Monte-Carlo Simulations Of Ion Release Curves (Brahim Mustapha and Jerry A. Nolen)

Studying nuclear structure at the limits of the chart of nuclides, especially near the proton and neutron drip-lines, requires high intensity radioactive beams not available at existing facilities. Since the most exotic nuclei have the shortest half-lives, the time from production to extraction (release) from the ion-source, called "delay time", has to be the shortest possible. The release process involves the transport of produced nuclei first through the target material (diffusion) then through the target chamber and ioniser (effusion). The aim of this work is first, to identify the dominant process in the release of a given isotope and second, to reduce the delay time in order to increase the efficiency of ISOL-targets to increase the intensities of rare isotope beams.

The delay time is a function of the radionuclide species, target material, geometry, and the experimental conditions. In this work, we are interested in optimizing the target geometry for a faster release. This concerns mainly, the thickness, shape and arrangements of the target material inside the target chamber. For this purpose, we are using a Monte-Carlo calculation where the geometry is implemented using Geant-4. Produced particles are followed individually from production to release. The delay time is computed event by event. All processes involved: diffusion, effusion and decay are included to obtain the overall release curve.

Description of the Calculation

Since the shape and dimensions of the target could help in making the release faster, it is very important to be able to choose the target geometry in order to minimize the delay time. Using the power of the tool kit Geant-4[1], it is possible to implement any complicated 3D-geometry and modify it easily. The diffusion and effusion processes are treated separately. The diffusion is treated analytically using the Kirchner formula[2], a solution of Fick's equation. The formula gives the probability for a particle to diffuse out of the target foil at a time t. The diffusion is characterized by the time $\tau_d = \dfrac{d^2}{\pi^2 . D}$ at which about 70% of particles have left the target material. d is the thickness of the target foils and D is the diffusion coefficient, a function of particle/target properties and the temperature. The formula is randomized to generate the diffusion time t_{df} event by event.

For the effusion, a special routine has been written and added to the list of physics processes of Geant-4. This new process considers the thermal motion (Maxwell motion) of a particle inside the target volume and treats its collisions with the encountered surfaces. At each collision, the particle sticks to the surface (adsorption, Frenkel-equation[3]) is reemitted (desorption) to the target volume in a direction obeying the cosine distribution (Knudsen Law[4]). The calculation is stopped when the particle leaves the ioniser. For each event, the total path length and the number of collisions with the surface are computed. They are used respectively to determine the flight time and the total sticking time. The effusion time, t_{ef} is the sum of the flight and sticking times.

The total delay time is then obtained by adding the diffusion and effusion times: $t_{df} + t_{ef}$. At this stage, we have the delay time distribution before decay.

To consider the decay of nuclei while diffusing and effusing through the target and obtain the final release curve, the decay factor: exp $(-\lambda.t)$ is applied to the distribution of delay times.

RIST Target Simulation

The Radioactive Ion Source Test (RIST) target[5] was designed and constructed at Rutherford Appleton Laboratory, UK and tested at ISOLDE-CERN[6]. The target is a 20-cm-long, 2-cm diameter tantalum tube filled with 25μ-thick discs (3600 discs total). Discs have holes in the middle to let particles effuse through the target to a connection tube then to the ioniser.
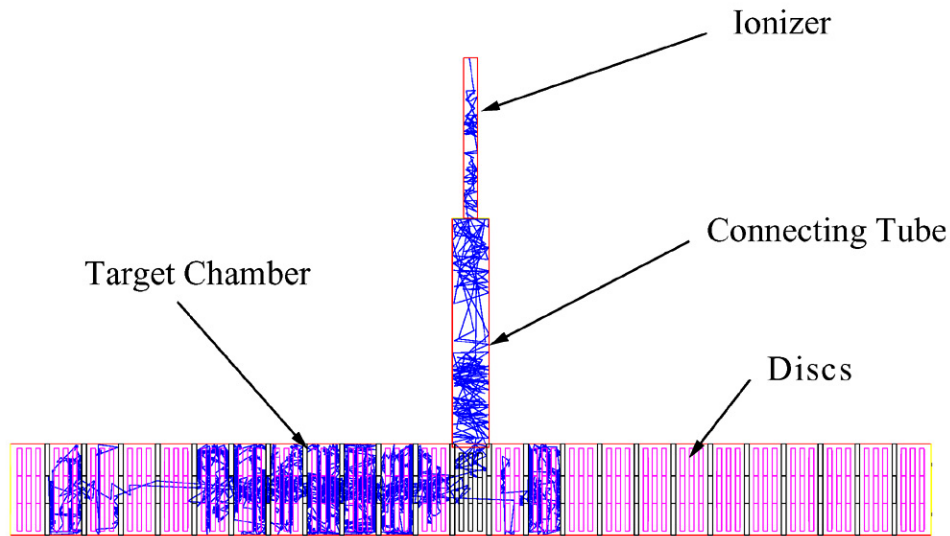
Fig. III-14. Geometry of the RIST target showing the path of one particle from production to release.

Earlier analysis of the release curves obtained with the RIST target at ISOLDE were presented in[7] and[8]. The present effort is to simulate this target with a detailed 3-D model using the Geant-4 tool kit described above. The simulation is performed for the experimental conditions at ISOLDE to study the release of ^{8}Li at a temperature of 1950° C. The result of the simulation is compared to the data in order to identify the dominant process in the release.

The result of the effusion part shows that particles collide more than 2×10^6 times with the target surface and travel 240 m on the average before exiting the ionsier. This corresponds to an average flight time of 95 ms. The sticking time and the diffusion coefficient (diffusion time) are free parameters to fit the data. Figure III-14 illustrates the target geometry and the effusion path of a single atom.

A good fit was obtained for a sticking time per collision τ_s = 0ns (or < 1ns) and any value of the diffusion coefficient D ≤ 10^{-7} cm^2/s. For example, using D of 10^{-8} cm^2/s gives exactly the same release curve as D of 10^{-7} cm^2/s after re-normalizing.   This lack of sensitivity of the release curve to the value of D beyond an upper limit D_s ~ 10^{-7} cm^2/s is due to the fact that the absolute normalization of the data is unknown. The

lifetime of ^{8}Li is too short to determine D without supplemental information from a longer-lived isotope (see below).

Considering D of 10^{-7} cm^2/s, we notice that a better fit of the release curve can be obtained by adding a faster diffusion component, representing only 3% of events, with D = 5×10^{-6} cm^2/s. This fast component may be due to hot spots in the target or an enhancement of the release during the very short beam pulse. The relative amount of the required fast component is less for shorter main components; e.g. it is only 1% for D of 10^{-8} cm^2/s. The calculated delay curve which corresponds to either of these cases is shown in Fig. III-15.

To better determine D, release data from stable isotopes measured over a longer time interval can be used. Using the value D = 10^{-8} cm^2/s obtained for the closest stable isotope ^{7}Li by R. Bennett et al[9], we estimated the release efficiency of the target for ^{8}Li to be about 8% which is mainly due to the very long diffusion time τ_d = 63.3 s compared to the ^{8}Li half life $T_{1/2}$ = 0.84 s. To increase the efficiency of the target we may use thinner discs. The simulation of the same target with 2.5μ discs results in an efficiency of about 65%, eight times more than the first configuration. This proves that by choosing the target geometry, it is possible to improve its efficiency in order to produce higher intensity radioactive beams and beams of very rare isotopes.
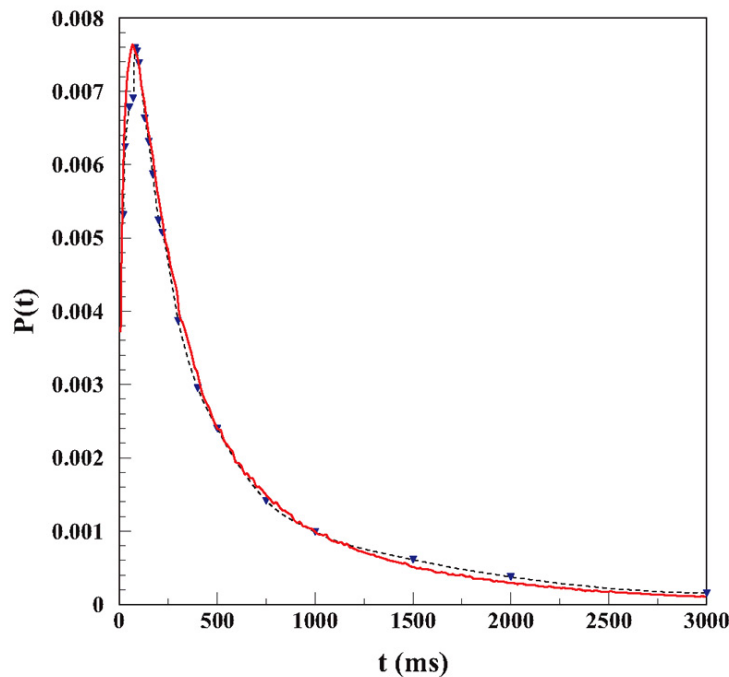
Fig. III-15. Best fit of ^8Li release curve, obtained with a sticking time <1ns and two diffusion components: 1% fast with $D = 5\times 10^{-6}$ cm^2/s and 99% slow with $D \leq 10^{-8}$ cm^2/s.

Conclusion and Future Plans

A general method for simulating release curves for ISOL targets has been developed. It is based on a standard analytical treatment of the diffusion of radioisotopes from the target material and a general Monte Carlo treatment of the effusion process from the target area to the ion source. Detailed 3-dimensional geometries for the effusion process are modeled by the C++ code Geant-4, and the ions are tracked via a new physics subroutine written for this code package. The limiting elements for the diffusion/effusion processes can be identified by this simulation model, leading to predictions for improvements in extraction times and overall efficiencies of the ISOL method. The Monte Carlo calculations for the RIST target geometry are time consuming on present Linux-based PC systems. The present calculations each took up to a week running as background jobs on a cluster of 10 such PC's. To speed up the process of optimizing ISOL target designs, we are planning to implement parallel processing for the Geant-4 package using the MPI method. This will permit such calculations to be carried out effectively on large parallel-processor computers such as the ANL 512-processor "Chiba-City" Linux cluster and/or the NERSC computers at LBNL.

[1] Geant4 home page : http://geant4.web.cern.ch/geant4/.

[2] R. Kirchner, NIM B 70 (1992) 186.

[3] R. Kirchner et al, NIM A 247 (1986) 265.

[4] M. Knudsen Ann. d. Phys. 48 (1915) 1113 (in German) and "Introduction to the Kinetic Theory of Gases" by Sir J. James (Cambridge University Press 1940).

[5] J. R. J. Bennett et al, NIM B 126 (1997) 117.

[6] P. V. Drumm et al, NIM B 126 (1997) 121.

[7] C. J. Densham et al, NIM B 126 (1997) 154.

[8] J. R. J. Bennett, Proceedings of RNB 2000.

[9] J. R. J. Bennett, private communication.

c.5.   Design Layout of an Isobar Separator for Purifying Beams of Rare Isotopes
(M. Portillo, J. A. Nolen, T. A. Barlow)

An important feature of the RIA facility is the filtering out of unwanted isotopes species from beams of rare isotopes obtained from ISOL sources. Much of this contamination is expected to stem from isobars of similar m/q or from mass tails of species whose intensities are very large compared to the isotope of interest. Simulations of a dual-potential mass separator have been carried out in designing a system that can purify such beams while maintaining high transmission. The design goal is to obtain 5 MeV mass separation at A=100, which is equivalent to a mass resolving power of $m/\Delta m \geq 20,000$. For such high mass resolutions it is necessary to minimize distortions caused by higher order aberration from the elements and the energy spread of the ions.

A solution based on magnetic separation at two energies is shown in Fig. III-16, where the beam is decelerated to in the second section to 90% of its incident energy. The beam enters the first section at point **A** at 100 keV and a 10π mm-mr emittance with an aspect ratio of xm/ym =1mm/8mm. The energy spread of the beam is taken to be ±10 eV relative to the reference particle. Two magnetic sectors of 60° bend with a radius of 2.5 m are paired in mirror symmetry with a multipole between them. Despite a mass dispersion of $(x,\delta m)$=23 m provided at point **C**, the masses are not resolved due

to the energy spread, as shown by the inset plot. By decelerating the beam and then bending in the opposite direction at the same dipole field strength, it is possible to obtain an achromatic solution. The resulting mass distribution is also shown on the inset to demonstrate that the energy spread effect is eliminated to first order by the time the beam exits at point **F**. The beam is then accelerated back to its original potential.

The calculations were carried out using the COSY INFINITY code sytem which utilizes differential algebraic techniques. The deceleration section assumes two immersion lenses with optimization of the potential at each gap to provide the necessary telescopic focusing. Fifth order calculations were sufficient for determining the necessary multipole strengths to minimize aberrations.

The plots in the inset have been obtained from simulations where phase space distributions of Gaussian character were assumed. The result is that for two masses separated in mass by $m/\Delta m$ =1/20,000 one expects a cross contamination of about 5% when 96% of the desired mass is accepted. Furthermore, impurities introduced by scattering of ions by residual gases should be largely eliminated by this multistage method.
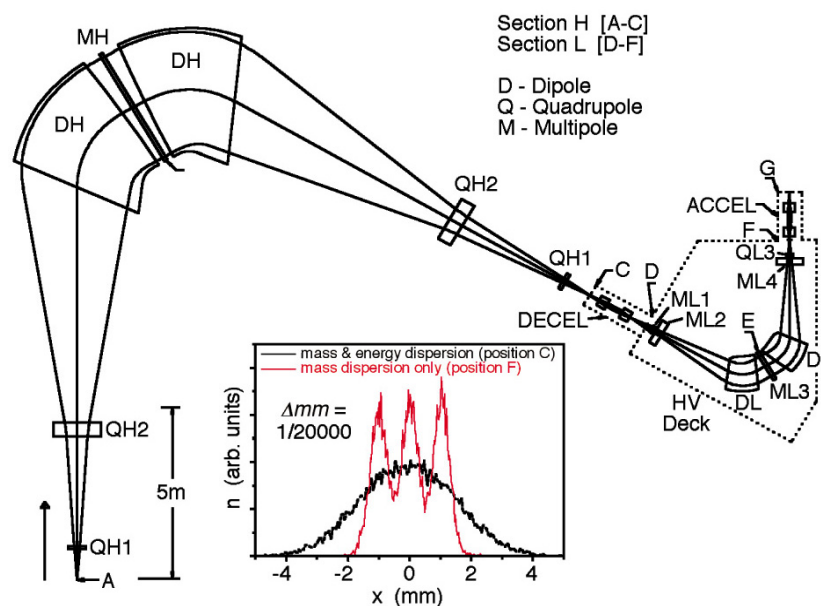

Fig. III-16. Layout of dual-potential spectrometer. The separation is split into multiple sections to obtain achromatic focusing. The inset shows a plot of the beam distribution at points C and F.

c.6.   Validation of Two-Step Target Simulations (M. Portillo, J. Nolen, I. Gomes, V. N. Panteleev*, D.V. Fedorov*, A.E. Barzakh*, V. I. Beznosjuk*, F.V. Moroz*, S.Yu. Orlov*, Yu. M. Volkov*)

The two-step reaction process for the production of rare isotopes in ISOL (Isotope Separation On Line) targets offers some advantages over the one-step configuration. In the one-step, a primary beam of high-energy particles, such as protons, directly impinges on the target. Most, if not all, of the power is then dissipated directly into the target. Estimates on the amount of production necessary for an intense rare isotope facility require that that at least 100 μA of protons at energies ranging from 0.5 to 1 GeV be directed on target. Studies in the past have predicted that conventional targets will not be able to sustain the type of power densities imposed under target conditions required for releasing rare isotopes.   The two-step geometry is proposed to produce intense yields of neutron-rich fission fragments while keeping the primary beam power out of the uranium target.   The present experiment was designed to test the Monte Carlo simulation of the production rates with a simplified 2-step geometry.

Especially in the case of producing neutron deficient isotopes, issues of target lifetimes and reliability require that alternative methods of production be considered. Others have proposed that for the case of neutron rich isotopes, it may be necessary to consider neutron-induced fission by fast neutrons on uranium instead of direct protons. The efficient production of fast neutrons on a primary target could be used to produce a sufficient amount of neutron flux to make the so called two-step production method a better alternative.   These two competing methods of production will be compared by measured and simulated production yields in the Rb and Cs mass region.

The experiment was conducted at the IRIS facility at Petersburg Nuclear Physics Institute.   The apparatus used allowed an immediate switching between a one-step and two-step mechanism setup for ease in comparing the final results.   The relative measurements obtained from this ISOL configuration offers a direct comparison between the two processes.

Monte Carlo calculations conducted at Argonne National Laboratory were used to interpret the results in more detail. They apply nuclear cascade models for predicting the production yields in each of the two configurations. Release curves were measured in order to characterize the efficiency of the IRIS target/ion source with a UCx target that was developed at the PNPI facility. These measurements were used to unfold the actual production yields at the target from the measured count rates at the exit of the mass separator system.

Measuring the ratio of the yields between the direct and indirect setup can be compared directly with the ratios predicted by the Monte Carlo simulations since the release efficiencies cancel out. The results obtained at both mass regions are shown in Fig. III-17 where (a) is for the neutron rich Rb mass region and (b) for the Cs. The agreement with the experimental results lends support to the nuclear model, which in turn predicts that neutron induced fission is a viable production mechanism. The Monte Carlo simulations have been used in the design of future high power targets based on the two-step method.
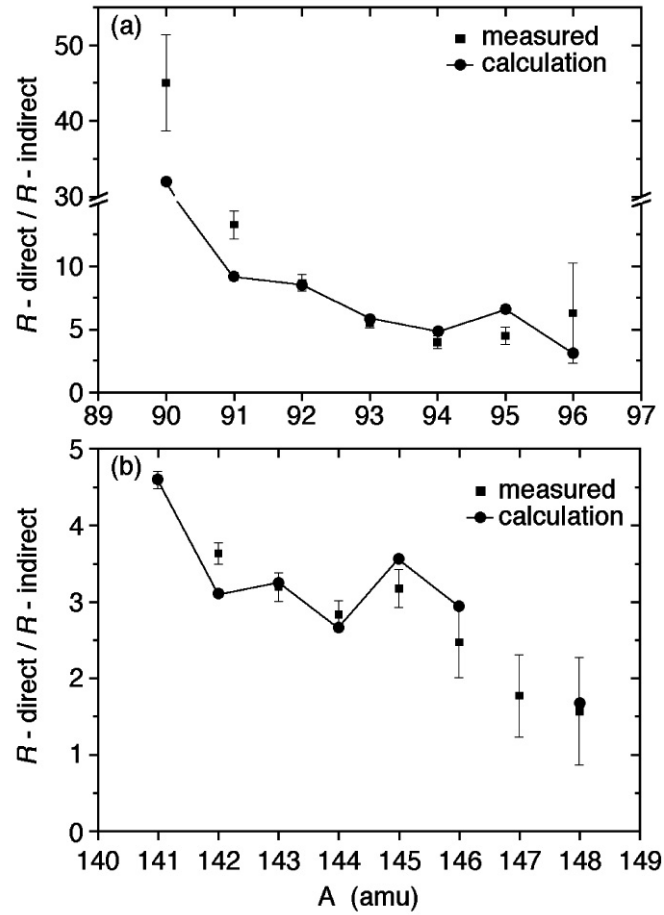
---

* IRIS, Petersburg Nuclear Physics Institute

Fig. III-17. The ratios of yields measured and predicted for direct relative to the indirect irradiations. Isotopes in the neutron-rich rubidium mass region are plotted in (a) while those of cesium are in (b).

D. RARE ISOTOPE BEAM DIAGNOSTICS

d.1. Design and Test of a Beam Profile Monitoring Device for Low-Intensity Radioactive Beams (P. N. Ostroumov, P. Billquist, M. Portillo and W. Q. Shen)

Development efforts have gone into the construction and performance testing of a device that can be used to provide snap shot images of the beam profile for very low intensities beams, such as those expected to be handled with the rare-isotope accelerator. Beam position and intensity analysis are among the most critical tools in tuning beams through linear accelerators and play a key role in the acceleration process. With the advent of a pepper pot plate, this system can be used to extract transverse emittance information of the beam for both the x-x' and y-y' phase space planes, simultaneously. Conventional diagnostic devices used in heavy ion accelerators for this purpose generally require at least 10^4 times more intensity than is expected for rare isotope beams to extract such information at the low energy regime (W<10keV/u).   At higher energies, particle detectors can be implemented, however, most of

them require extra features to obtain spatial information and lifetime sensitive to the destructive energy deposited by the beam. The device tested here was designed with these factors taken into consideration.

A lay-out of the measurement device is illustrated in Fig. III-18. The beam come in from the left and will pass through any necessary slits or apertures, such as the pepper pot plate. The beam of particles impinge on a plate acting as a conversion surface to convert the energy deposited by the particles into relatively slow secondary electrons.   This is essentially a stage of amplifying the amount of charge induced by the incident ion, since each ion can on average produce about 3 to 10 secondary electrons per ion, depending on the particles   incident   velocity   and   Z,   and   the
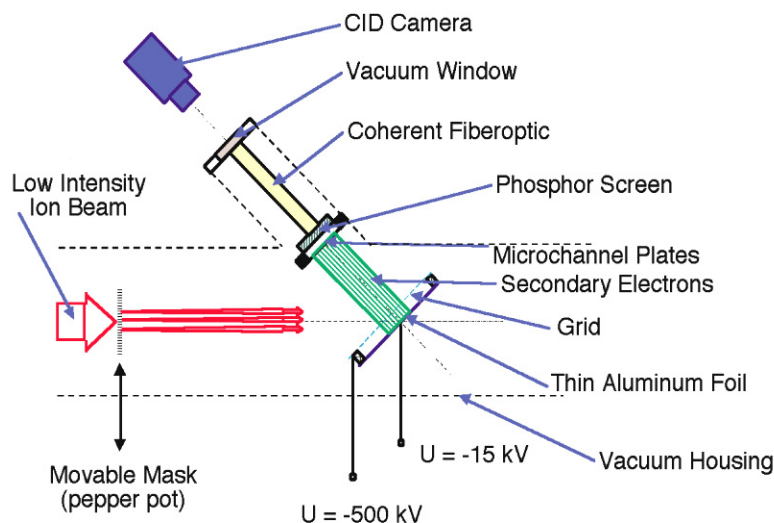

Figure III-18. Simplified layout of the device for measurement of transverse emittance and density distribution of low intensity radioactive beams.

chemical composition of the surface. The conversion surface is at 45 degrees relative to the beam's optic axis and is made of a flat piece of aluminum foil which is under negative high voltage up to –15 kV.   The secondary electrons are accelerated through a ~10 kV

potential with a grid that is parallel to the conversion surface to minimize the divergence of the emitted electrons. The accelerated secondary electrons strike a region of a microchannel plate facing parallel to the conversion surface. Along with another similar MCP

lying right behind the first, the signal from the secondary electrons can be amplified by as much as a factor of 10^9 times. The pulse of electrons generated at the back of the MCP are then accelerated through a 4 kV potential over a 5 mm even spacing between the MCP surface and an aluminum coated phosphor screen. The light emitted by the excitations induced by the accelerated electrons and the phosphor screen are then transported through sections of rods made of tightly packed optic fibers. The light signals arrive at a 2-D array of light sensitive detectors, known as the charged integrating device (CID). The position on the CID at which the light signal arrives is directly related to the position where the particle initiating the signal strikes on the conversion surface.

The conversion surface hangs from a linear feed through device and may be moved to the top of the vacuum vessel to allow the beam to pass. Figure III-19(a) has a photograph of the outside of the vacuum vessel to illustrate the position of the pepper pot feed through and the position of the detection system located 30 cm behind it. Figure III-19(b) has a photograph of the inside of the vacuum vessel illustrating the back of the conversion surface as it is pulled half-way out. A partial view of the front of the MCP can be seen.

Recent tests with $^{84}Kr^{1+}$ ions from the Dynamitron accelerator have shown that a beam 3.6 keV/u or 12 keV/u can be well resolved down to an intensity of about 10^4 pps. A normalized intensity distribution is plotted along the horizontal and vertical dimensions of the conversion surface as illustrated in Fig. III-20. The beam was attenuated with fine mesh grids while the pepper pot plate was out of the way. A 1.4% efficient channeltron detector was used to monitor the intensity of the beam from a position farther up-stream from the detection system. The image from the CID has been processes with an 8-bit resolution ADC which can acquire up to 30 frames per second. A bitmap image of a single snap shot is illustrated in Fig. III-20.

At present the detection device has shown promising results for processing images of low intensity beam profiles. In fact, as is seen from Fig. III-21 a location of individual ion can be monitored. It indicates that the device is applicable in full range of RIB beam intensities from several particles per second to 10^{11} pps. Improvements to the data acquisition system are underway to process the data and acquire emittance profiles from the pepper pot grid. At this point it has been proven that such a device is sensitive to low energy beams. At higher incident energies the particles produce sufficient amount of secondary electrons on the conversion surface, making it efficient for beams up to ~10 MeV/u. Thus, this device should be well suited for the entire spectrum of particle energies expected for accelerated rare isotope beams. Since the MCP plates are highly insensitive to gamma radiation and the distance to the conversion surface is over 8 cm, this detection system is expected to be sufficiently immune to radioactive decay of the implanted particles. For higher energy particles, the foil may even be thin enough to allow full penetration, which further favors this configuration. Future tests are intended to characterize these features, and allow further assessments.

(a)

HV Cable

"Pepper pot"
Feed Through

Foil
Feed Through
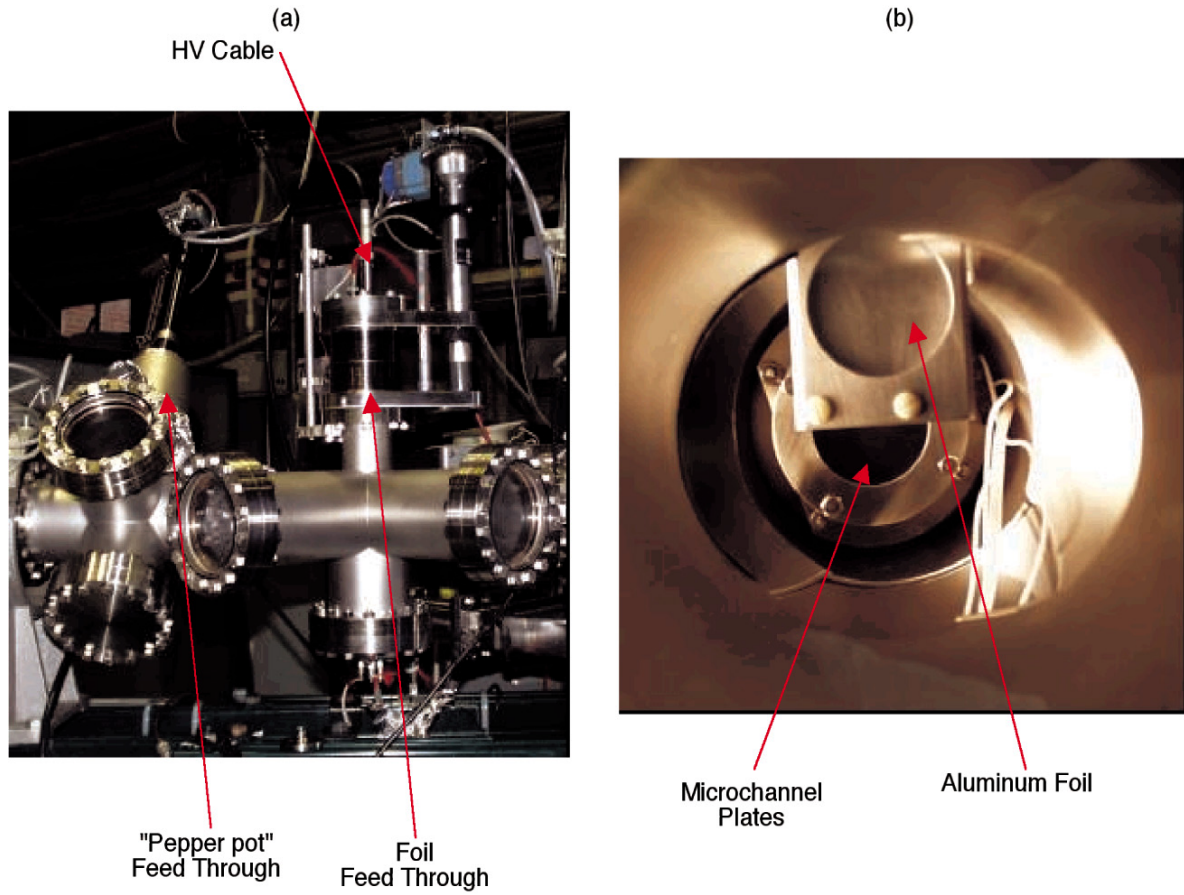
(b)

Microchannel
Plates

Aluminum Foil

Figure III-19. Side view of the detector on Dynamitron beam line (photo in the left) and internal view of the aluminum foil and microchannel plate (photo in the right).
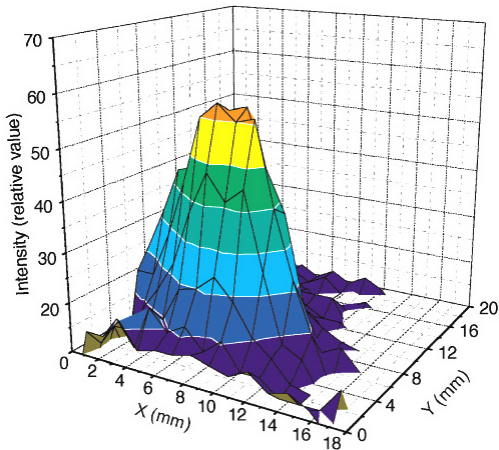
Figure III-20. Beam density distribution in transverse plane. Foil voltage is -11 kV. Beam intensity is ~10^{10} pps.
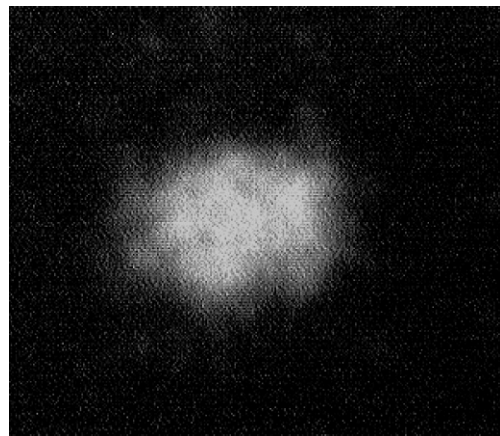
Figure III-21. Low intensity krypton ($2 \cdot 10^4$ pps) beam image as is seen on PC screen. Beam size is ~4x3 mm·mm.